Inorg. Chem. **1981**, *20*, 1403-1409 **1403**

Contribution from the Department of Chemistry,
University of Washington, Seattle, Washington 98195

Electronic Structure of Iron Complexes Containing Extended Ligand π Systems[1a]

JOE G. NORMAN, JR.,*[1b] LUANN M. L. CHEN, CHRISTOPHER M. PERKINS, and NORMAN J. ROSE

Received November 13, 1980

SCF–Xα–SW calculations have been carried out for $N_2C_2H_4$, NCS^-, $Fe(N_2C_2H_4)_2(NCS)_2^{0,+}$, and $Fe(N_2C_2H_4)_2(SCN)_2^+$, where NCS^- is coordinated to iron through nitrogen in the first two complexes and through sulfur in the third. $N_2C_2H_4$ is the simplest possible α-diimine, a model for TIM, which is a 14-membered macrocycle containing two α-diimine moieties. The calculations predict that the electron removed upon oxidation of $FeTIM(NCS)_2$ to $FeTIM(NCS)_2^+$ or $FeTIM(SCN)_2^+$ comes from a mainly NCS^- 2π orbital. The oxidized complexes are therefore best represented formally as Fe(II) and two $NCS^{0.5-}$ radicals. The NCS^- fraction of the radical character is mostly on the sulfur atoms. The mainly 2π HOMO's of the three complexes lie between the filled dπ and empty dσ orbitals in energy. The observed easy interconversion between $FeTIM(NCS)_2^+$ and $FeTIM(SCN)_2^+$ is discussed in terms of the calculated orbitals; a weak Jahn–Teller instability of the N-coordinated isomer is noted. Low-lying $N_2C_2H_4$ C–N π^* orbitals are found essentially coincident with the Fe dσ orbitals in energy, implying that reduction of $FeTIM(NCS)_2$ could produce an Fe(II) species containing TIM radical anion.

The 14-membered macrocycle **1**, known as TIM for short,

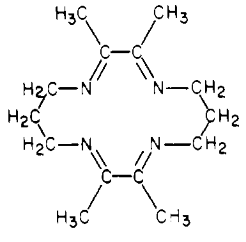

1

coordinates strongly to metals such as Fe, Co, Ni, and Cu, always in a planar fashion. The resulting robust M(TIM) units can bind a wide variety of axial ligands to form five- and six-coordinate complexes.[2-8] Particularly well studied are $FeTIM(X)(Y)^{n+}$, which exist for both Fe(II) and Fe(III).[3-7] They are always low spin, reflecting the strong bonding of the TIM. Complexes containing axial ligands ranging from Cl^- to CO—and including CH_3CN, imidazole, and NCS^-—have been characterized.

An interesting outcome of this work has been the discovery that $FeTIM^{2+}$ is a homogeneous catalyst for the photooxidation of methanol to formaldehyde.[6] The catalytic cycle (1) takes

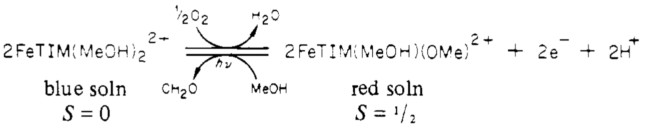

$$2FeTIM(MeOH)_2{}^{2+} \underset{h\nu;\ CH_2O,\ MeOH}{\overset{\frac{1}{2}O_2,\ H_2O}{\rightleftharpoons}} 2FeTIM(MeOH)(OMe)^{2+} + 2e^- + 2H^+ \tag{1}$$

place at room temperature and atmospheric pressure merely upon alternate exposure of a methanol solution of the complex to air and sunlight. The stability of both Fe(II) and Fe(III) forms of the complex and their ease of interconversion are obviously vital to the success of the catalysis. An intriguing possibility is that this stability and ease of interconversion are at least partly due to significant axial ligand character in the highest occupied orbitals, which would normally be of dπ type. The methoxide would be then already partially oxidized in the ground state of the *formally* Fe(III) complex, and the redox process would not perturb the metal center as much as a normal Fe(II)–Fe(III) interconversion.

Table I. Magnetic Properties of "Fe(III)" Complexes of TIM[a]

complex	χ_M, cgsu × 10^3	$\mu_{eff}{}^{cor}$, μ_B	stability of Fe(II) complex
$[FeTIMCl_2]PF_6$	1.49	2.04	unstable
$[FeTIM(SCN)_2]PF_6$	1.32	1.95	stable
$[FeTIM(SCH_2Ph)_2]PF_6$	1.10	1.87	unknown

[a] From ref 7. Each complex has one unpaired electron.

There is in fact physical evidence for considerable ligand character in the highest occupied orbitals of FeTIM complexes. The magnetic moments of three formally Fe(III) complexes are shown in Table I. They are all below the typical value of 2.3 μ_B for this oxidation state, lying toward the 1.73 μ_B expected if the unpaired electron were localized on the ligands. The thiocyanate complex, alone among the three, is easily worked with at both oxidation levels. This is reminiscent of the catalytic system, with the additional virtue that both Fe(II) and "Fe(III)" forms are isolable as crystalline solids. A natural question is what effect the extended π system of NCS^-, absent for Cl^- and $PhCH_2S^-$, has on the observed stability.

We have carried out SCF–Xα–SW calculations on the models for $FeTIM(NCS)_2^{0,+}$ shown in **2**, which have D_{2h}

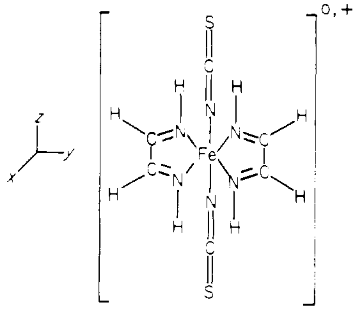

2

symmetry. Our main goals were to determine the nature of the orbital which loses the electron upon oxidation and the extent of interaction between Fe dπ and ligand π orbitals. The latter question is of interest for TIM as well as NCS^-; the

---

(1) (a) Presented in part at the 177th National Meeting of the American Chemical Society, Honolulu, April 1979; see Abstracts, No. INOR-509. (b) Fellow of the Alfred P. Sloan Foundation, 1978-1980.

(2) (a) Jackels, S. C.; Farmery, K.; Barefield, E. K.; Rose, N. J.; Busch, D. R. *Inorg. Chem.* **1972**, *11*, 2893. (b) Dabrowiak, J. C.; Merrell P. H.; Stone, J. A.; Busch, D. H. *J. Am. Chem. Soc.* **1973**, *95*, 6613.

(3) Baldwin, D. A.; Pfeiffer, R. M.; Reichgott, D. R.; Rose, N. J. *J. Am. Chem. Soc.* **1973**, *95*, 5152.

(4) (a) Smith, H. W.; Santasiero, B. D.; Lingafelter, E. C. *Cryst. Struct. Commun.* **1979**, *8*, 49. (b) McCandlish, L. E.; Santasiero, B. D.; Rose, N. J.; Lingafelter, E. C. *Acta Crystallogr., Sect. B* **1979**, *B35*, 3053.

(5) Incorvia, M. J.; Zink, J. I. *Inorg. Chem.* **1977**, *16*, 3161; **1978**, 17, 2351.

(6) Reichgott, D. W.; Rose, N. J. *J. Am. Chem. Soc.* **1977**, *99*, 1813.

(7) Fey, E. O. Ph.D. Thesis, University of Washington, 1979.

(8) Maroney, M.; Rose, N. J.; Lingafelter, E. C., unpublished results ($CuTIM^{2+}$ complexes).

0020-1669/81/1320-1403$01.25/0

extent of metal d$\pi \rightarrow$ imine π^* back-donation has been a point of discussion in the chemistry of α-diimine complexes for many years.[9]

No crystal structures were available for these complexes when we began the calculations. Our choice of the N-bonded thiocyanate isomers was based on the infrared spectra.[7] FeTIM(NCS)$_2$ exhibits a strong, sharp ν(C–S) at 800 cm^{-1}, a reasonable indication of N coordination. For [FeTIM(NCS)$_2$]PF$_6$ this region of the spectrum is obscured by PF$_6$ absorption. A tentative indication of N coordination in the cation is that ν(C–N) values for both complexes are identical (2105 cm^{-1}). Given this and the hard–soft acid–base concept that Fe(III) would prefer N over S coordination even more than would Fe(II), we assumed that both complexes contained N-bonded thiocyanate.[7]

When our calculations on **2** were nearly complete, the crystal structure of the cationic complex became available, revealing that it in fact contains S-bonded thiocyanate in the solid.[10] Subsequent new infrared studies suggest that an equilibrium exists between N- and S-bonded isomers in solution.[11] Moreover, recent flash photolysis experiments on solutions of the Fe(II) complex, almost certainly N bonded in the ground state, indicate that upon photochemical excitation a metastable S-bonded isomer is generated.[12]

We therefore decided to extend our calculations to include **3**, which has C_{2h} symmetry. We hoped from comparison of the calculated electronic structures of all three models to find a simple reason, and perhaps a mechanism, for the easy interconversion between N- and S-bonded isomers of the oxidized or photoexcited complex. For purposes of comparison, we also calculated the free ligands NCS$^-$ and N$_2$C$_2$H$_4$.

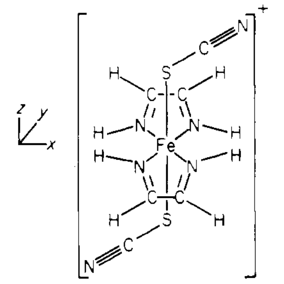

3

Computational Section

Dimensions of the Fe(N$_2$C$_2$H$_4$)$_2$ fragments in Fe(N$_2$C$_2$H$_4$)$_2$(NCS)$_2{}^{0,+}$, and of free N$_2$C$_2$H$_4$, were taken from the crystal structure of [FeTIM(NCCH$_3$)$_2$][PF$_6$]$_2$,[4a] with C–H = 1.05 and N–H = 1.00 Å. The C–N and C–S distances for the N-bonded thiocyanates, and for free NCS$^-$, were 1.16 and 1.64 Å, respectively, an average of literature values for N-bonded complexes. The Fe–NCS distance was 1.929 Å, the same as the Fe–NCCH$_3$ distance in [FeTIM(NCCH$_3$)$_2$][PF$_6$]$_2$. Dimensions for Fe(N$_2$C$_2$H$_4$)$_2$(SCN)$_2{}^+$ were taken from its crystal structure;[10] in particular, the Fe–S–C angle was 104°. The Fe(SCN)$_2$ plane was erroneously taken as *xz* (see **3**) rather than *yz* as in the actual structure; this does not significantly affect conclusions drawn from the calculation (see Discussion).

The initial molecular potentials for NCS$^-$, N$_2$C$_2$H$_4$, Fe(N$_2$C$_2$H$_4$)$_2$(NCS)$_2{}^+$, and Fe(N$_2$C$_2$H$_4$)$_2$(SCN)$_2{}^+$ were constructed by superposition of atomic SCF–Xα charge densities. Overlapping-sphere radii for these species were chosen by our nonempirical procedure[13] as 88% of the atomic-number radii. For NCS$^-$ and Fe(N$_2$C$_2$H$_4$)$_2$(SCN)$_2{}^+$ "Watson spheres"[14] of opposite charge were used to simulate lattice and solvation effects. The SCF calculation for Fe(N$_2$C$_2$H$_4$)$_2$(NCS)$_2$ was started from the converged potential for Fe(N$_2$C$_2$H$_4$)$_2$(NCS)$_2{}^+$; one electron was added to the single half-filled energy level of the cation, and the potential was shifted uniformly upward to remove the effect of the positive charge. The same sphere radii were maintained. Table II lists the sphere radii used for all molecules.

Table II. Atomic and Outer-Sphere Radii (bohr radii)

region	NCS$^-$	N$_2$C$_2$H$_4$	Fe(N$_2$C$_2$H$_4$)$_2$-(NCS)$_2{}^{0,+}$	Fe(N$_2$C$_2$H$_4$)$_2$-(SCN)$_2{}^+$
outer	4.941	5.615	11.334	9.376
Fe			2.253	2.303
N(TIM)		1.694	1.663	1.663
C(TIM)		1.655	1.671	1.671
H$_{\mathrm{N(TIM)}}$		1.151	1.155	1.155
H$_{\mathrm{C(TIM)}}$		1.249	1.261	1.261
N(NCS)	1.659		1.661	1.682
C(NCS)	1.603		1.624	1.623
S	2.351		2.397	2.363

For the complexes the charge density and potential were corrected for double counting of charge in the sphere-overlap regions;[13,15] the calculations for the free ligands, done at an earlier time, do not include this correction. The main effect of such a correction is a uniform downward shift of the orbital energies; we compensate for its absence in the free-ligand calculations by uniformly shifting their levels downward so that the energies of low-lying noninteracting ligand orbitals are equal in the ligands and complexes (see Results, specifically caption to Figure 1). Similarly, we facilitate comparison of the orbital energies of the complexes by uniformly shifting the levels of the cations to make the energies of low-lying N$_2$C$_2$H$_4$ levels the same for all three species, thereby approximately removing effects of the positive charges and Watson sphere (see Results, specifically footnote *b* to Table IV).

In other respects the calculations were carried out as previously described.[16] For the cationic complexes, several possible ground-state configurations (each with one half-filled orbital) were converged to determine the one that had the lowest total energy.

Results

Figure 1 shows the calculated valence energy levels of the free ligands NCS$^-$ and N$_2$C$_2$H$_4$. The important levels for consideration of bonding in the complexes are those above –0.6 hartree. Electrons in lower orbitals constitute the internal σ-bond framework of the ligand in question. Table III shows the representations of D_{2h} and C_{2h} to which the fragment symmetry-adapted orbital combinations involved in bonding belong. The important points are that (1) in the D_{2h} complexes, the main σ donation from N$_2$C$_2$H$_4$ and NCS$^-$ to the metal occurs in b$_{1g}$ (to d$_{xy}$) and a$_g$ (to d$_{z^2}$) representations, respectively, (2) in the D_{2h} complexes, interaction of ligand π with metal dπ orbitals occurs in b$_{2g}$ (with d$_{xz}$) and b$_{3g}$ (with d$_{yz}$) representations, and (3) in the C_{2h} complex, the bending of the Fe–SCN axis at sulfur allows interaction (in a$_g$ symmetry) of mixed SCN$^-$ σ and π orbitals with mixed Fe d$_{xz}$ and d$_{z^2}$ orbitals in the Fe(SCN)$_2$ plane, while perpendicular to this plane the interaction (in b$_g$ symmetry) is still between pure SCN$^-$ π and Fe d$_{yz}$ orbitals.

Table IV gives the energies and charge distributions of the upper valence orbitals in the complexes, i.e., those which correlate with the ligand orbitals above –0.6 hartree in Figure 1 and with the Fe 3d orbitals. The charge distributions of the corresponding free-ligand orbitals are also given for comparison. The listing in Table IV is by type, rather than strictly in order of energy; an energy diagram of the higher lying orbitals of the three complexes appears as Figure 2. Wave-function contour maps of critical orbitals for Fe(N$_2$C$_2$H$_4$)$_2$(NCS)$_2$ and NCS$^-$ are shown in Figure 3 and for Fe(N$_2$C$_2$H$_4$)$_2$(SCN)$_2{}^+$ in Figures 4 and 5.

---

(9) Krumholz, P. *Struct. Bonding (Berlin)* **1971**, 9, 139.
(10) Stenkamp, R.; Jensen, L. H., personal communication.
(11) Maroney, M., personal communication.
(12) Ferraudi, G. *Inorg. Chem.* **1979**, *18*, 1577.
(13) Norman, J. G., Jr. *Mol. Phys.* **1976**, *31*, 1176.
(14) Watson, R. E. *Phys. Rev.* **1958**, 14, 1108.
(15) (a) Herman, F. *Electrons Finite Infinite Struct.* **1977**, 382–410. (b) Yang, C. Y.; Johnson, K. H. *Int. J. Quantum Chem.* **1976**, *10S*, 159.
(16) Normal, J. G., Jr. *Inorg. Chem.* **1977**, *16*, 1328.

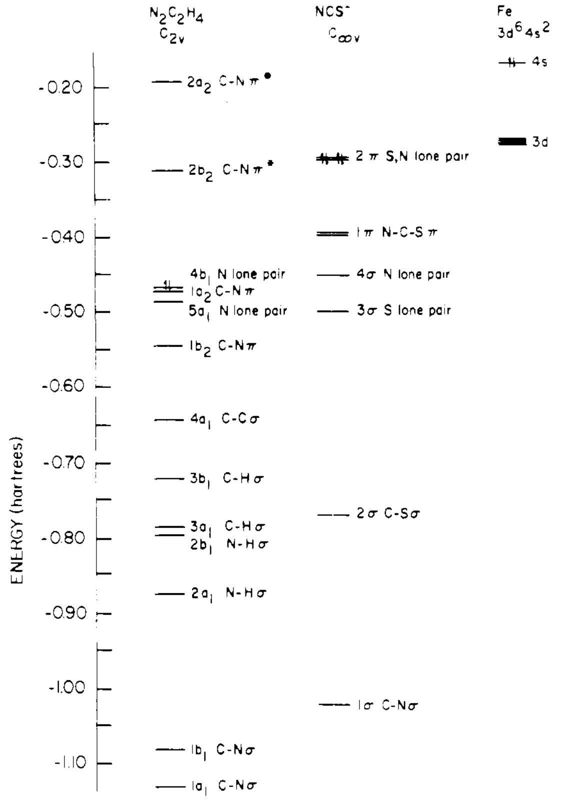

Figure 1. SCF valence energy levels for $N_2C_2H_4$, NCS^-, and Fe. The occupation of the highest occupied orbital for each species is shown, and the main character of the ligand orbitals is indicated. The energies for $N_2C_2H_4$ are 0.26 hartree lower than computed, making the average for those below −0.6 hartree equal to the average for the corresponding levels in $Fe(N_2C_2H_4)_2(NCS)_2$. The energies for NCS^- are 0.13 hartree lower than computed, making the 2σ energy equal to that of its counterpart in $Fe(N_2C_2H_4)_2(NCS)_2$. The molecular plane for the $N_2C_2H_4$ calculation was *xy*, with the C_2 axis along *y*.

Table III. Distribution of Fe, NCS^-, and $N_2C_2H_4$ Fragment Basis Functions Among Representations of D_{2h} and C_{2h}[a]

representations				
D_{2h}	C_{2h}	Fe	$(NCS)_2$[b]	$(N_2C_2H_4)_2$[c]
a_g	a_g	s, d_{z^2}, $d_{x^2-y^2}$	$\sigma + \sigma$	$\sigma + \sigma$ (a_1)
b_{1g}	b_g	d_{xy}		$\sigma^* - \sigma^*$ (b_1)
b_{2g}	a_g	d_{xz}	$\pi + \pi$	$\pi^* + \pi^*$ (a_2)
b_{3g}	b_g	d_{yz}	$\pi + \pi$	$\pi - \pi$ (b_2)
a_u	a_u			$\pi^* - \pi^*$ (a_2)
b_{1u}	b_u	p_z	$\sigma - \sigma$	$\pi + \pi$ (b_2)
b_{2u}	a_u	p_y	$\pi - \pi$	$\sigma - \sigma$ (a_1)
b_{3u}	b_u	p_x	$\pi - \pi$	$\sigma^* + \sigma^*$ (b_1)

[a] The coordinate system is that shown in 2 and 3 in the text. [b] Here σ and π refer to the symmetry with respect to the SCN–Fe–NCS axis of orbitals on individual NCS^- groups. Note that there is no differentiation between orbitals which are bonding and antibonding *within* individual NCS^- groups. [c] Here σ and σ* refer to in-plane orbitals on individual $N_2C_2H_4$ groups which are respectively symmetric and antisymmetric with respect to the C_2 axis. Similarly, π and π* refer to out-of-plane p-orbital combinations that are respectively symmetric and antisymmetric with respect to the C_2 axis. Again, there is no differentiation between orbitals which are C–N bonding and antibonding *within* individual $N_2C_2H_4$ groups. The representations of C_{2v} to which individual $N_2C_2H_4$ orbitals belong are given in parentheses.

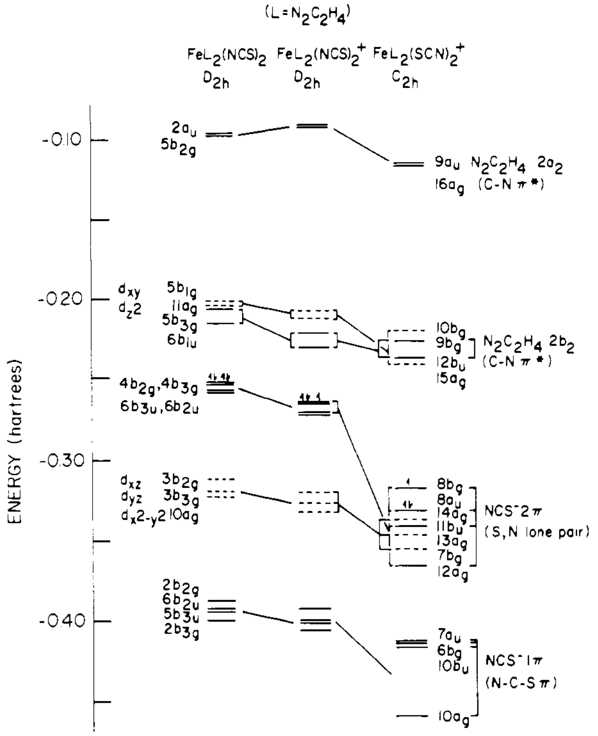

Figure 2. Frontier orbitals of the neutral N-bonded, cationic N-bonded, and cationic S-bonded complexes. The number of electrons in the highest occupied orbitals is shown. The Fe 3d, NCS^- π, or $N_2C_2H_4$ π* level with which each orbital most closely correlates is indicated. The d-like orbital energies are drawn as dashed lines; the ligand-like orbital energies, as solid lines.

We comment briefly here on our use of model rather than actual complexes and of our use of dimensions from crystal structures of similar molecules where none are available for the actual complexes. The substitution of hydrogen atoms for alkyl groups along the TIM backbone will have a first-order effect only on low-lying ligand σ orbitals, i.e., those below −0.64 hartree in Figure 1. We confine our discussion in this paper to the metal–ligand π interactions, i.e., to those orbitals above −0.55 hartree. Our long experience as both crystallographers and quantum chemists, coupled with careful analysis of the available data, convinces us that the actual dimensions of the complexes modeled are close to those used and that whatever small differences there are do not significantly affect our (largely qualitative) conclusions. If our modeling and dimensions were seriously in error, we would not expect the close agreement between experimental and calculated ligand field splittings noted in the following section.

Discussion

The calculations reveal interesting, but unsurprising, details of the metal–ligand σ interactions. These may be deduced from Tables III and IV and Figure 1; we confine our discussion to the π system.

Nature of the HOMO. Free NCS^- has three pπ levels, each degenerate. The lowest orbitals, 1π, are all bonding, and the highest, unoccupied 3π, are all antibonding. The intermediate 2π orbitals, the HOMO's of the ion, are approximately nonbonding (they would be completely so in a linear XY_2 molecule) and constitute sulfur and nitrogen lone pairs. Our NCS^- calculations (see Figures 1 and 3 and Table IV) show that the 1π electrons are evenly distributed over the three centers, while the 2π are about two-thirds on sulfur and one-third on nitrogen. The predicted charge distribution is thus closer to the

$$^{-}:\overset{..}{N}=C=\overset{..}{S}:$$

than to the

$$:N\equiv C-\overset{..}{\underset{..}{S}}:^{-}$$

resonance structure, although both contribute significantly.

The 3π level is at such high energy, +0.16 hartree on the scale of Figure 1, that dπ → 3π back-donation is not significant

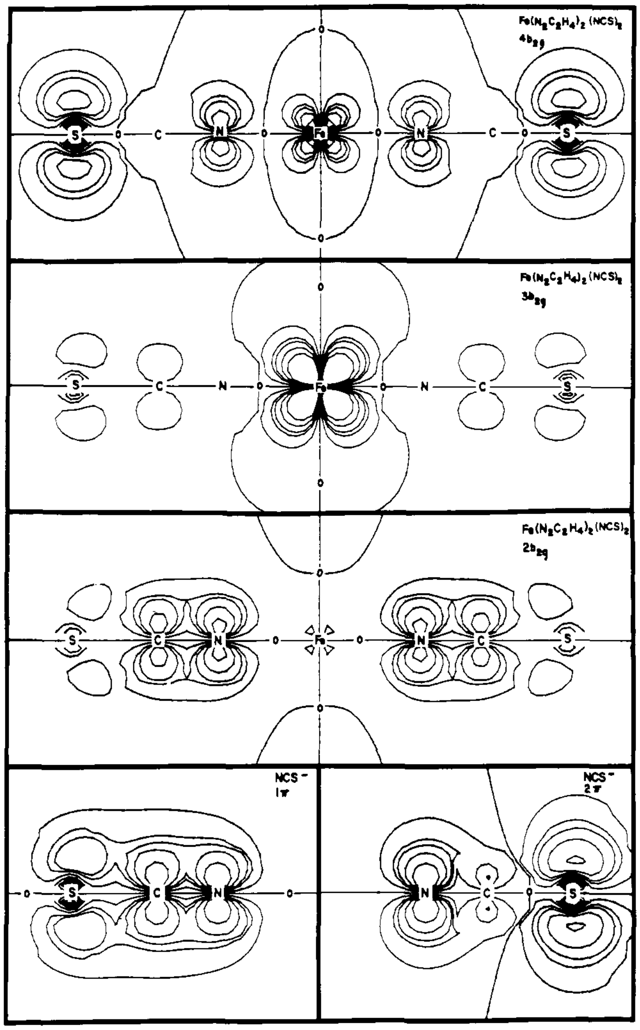

Figure 3. Contour maps of the 1π and 2π orbital wavefunctions for NCS^- and of mainly 1π, Fe $d\pi$, and 2π orbital wavefunctions of $Fe(N_2C_2H_4)_2(NCS)_2$ in the *xz* plane. Maps of the analogous orbitals of $Fe(N_2C_2H_4)_2(NCS)_2^+$ are similar, as are those of the $2b_{3g}$, $3b_{3g}$, and $4b_{3g}$ orbitals of both complexes in the *yz* plane. $4b_{2g}$ is the orbital which loses the electron upon oxidation. The contour values in this and subsequent maps are 0, 0.04, 0.08, 0.10, 0.14, and 0.20 $(\text{electron}/a_0^3)^{1/2}$. The zero contours are labeled to indicate changes of sign of the wavefunction. A change of sign between two centers indicates an antibonding interaction between them; no change of sign, a bonding interaction.

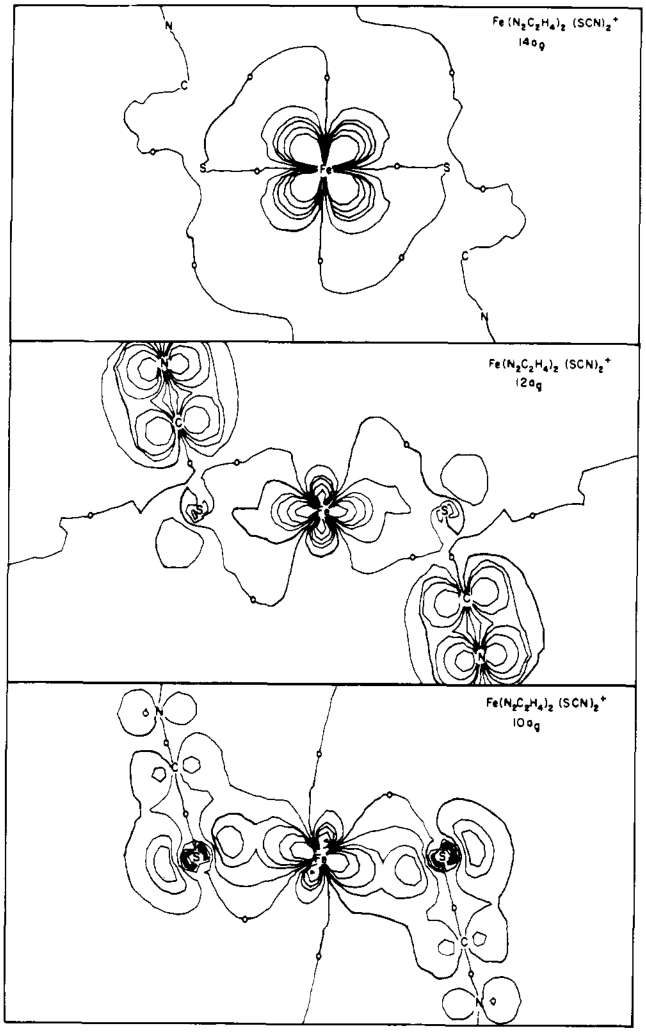

Figure 4. Contour maps of the orbital wavefunctions of $Fe(N_2C_2H_4)_2(SCN)_2^+$ in the *xz* plane which most directly correlate with those of $Fe(N_2C_2H_4)_2(NCS)_2$ in Figure 3. The correlation is $2b_{2g} \rightarrow 10a_g$, $3b_{2g} \rightarrow 14a_g$, and $4b_{2g} \rightarrow 12a_g$. Note that none of the orbitals shown here contains the unpaired electron (see Figure 2).

in the complexes. The 2π orbitals, however, are at comparable energy to the 3d manifold. The result is that the 2π analogues are the HOMO's of the complexes, lying between the filled $d\pi$ and empty $d\sigma$ orbitals, which are split by ca. 0.12 hartree (2.6 μm^{-1}) by the ligand field (see Figure 2). We note in passing that this predicted splitting is essentially the same as that derived from experiments (2.4–2.8 μm^{-1}) for low-spin Fe(II) and Co(III) complexes of TIM.[2]

The electron removed upon oxidation of the neutral complex to the cation is thus predicted to come from a mainly NCS^- π lone pair rather than from an Fe $d\pi$ orbital. In both N-bonded complexes, this orbital ($4b_{2g}$; see Table IV) has about 75% S, 15% N, and only 10% Fe character. In the S-bonded complex the proximity of sulfur to iron lowers the energy of the mainly sulfur 2π manifold, to the point where it overlaps the $d\pi$ levels in energy. Mixing between the two sets is therefore greater, and the orbital containing the unpaired electron ($8b_g$) is now about 45% S, 5% C, 20% N, and 30% Fe. The best formal representation of both oxidized complexes is thus Fe(II) and two $NCS^{0.5-}$ radicals rather than Fe(III) and two NCS^-. Note, however, that in the S-bonded complex the *single* atom with greatest unpaired electron density is iron, though the two sulfur atoms *together* have slightly more than the iron.

Wavefunction contour maps reveal details of the Fe–NCS π interactions. In Figure 3 the correlation with fragment orbitals is $2b_{2g} \rightarrow 1\pi$, $3b_{2g} \rightarrow d\pi$, and $4b_{2g} \rightarrow 2\pi$, the last being the orbital which loses the electron upon oxidation (see also Table IV). The 1π-like orbitals are seen to be polarized toward the metal upon complexation, losing most of their sulfur character. Conversely, the 2π lone pairs gain sulfur character at the expense of nitrogen and carbon character. The $d\pi$ orbitals mix only weakly with their ligand counterparts; there is certainly little net charge transfer, since the interacting orbitals on both centers are filled. The oxidation–reduction is easy because the electron exchanged comes from a largely nonbonding orbital delocalized over five centers; no bond or atom suffers a major perturbation. This is reflected in the calculated charge distributions by the lack of appreciable differences in character between analogous orbitals of the N-bonded neutral and cationic complexes.[17]

N vs. S Bonding of NCS^-. Comparison of Figures 3 and 4 reveals that interesting changes in the nature of certain 1π-

---

(17) There are some small differences in orbital mixing; e.g., $8a_g$ is purely $Fe-N_2C_2H_4$ bonding and $9a_g$ purely NCS^- 3σ lone pair in $Fe(N_2C_2H_4)_2(NCS)_2$, while in $Fe(N_2C_2H_4)_2(NCS)_2^+$ each of these two orbitals contains some of both types of character.

Table IV. Upper Valence Energies (hartrees) and Charge Distributions for Iron Complexes, Correlated with Those of Free Ligands[a]

$Fe(N_2C_2H_4)_2(NCS)_2$								$Fe(N_2C_2H_4)_2(NCS)_2^+$							$Fe(N_2C_2H_4)_2(SCN)_2^+$								$N_2C_2H_4$			NCS^-			
		% charge[d]							% charge[d]								% charge[d]							% charge[d]			% charge[d]		
D_{2h} level	energy	Fe	4NH	4CH	2N	2C	2S	energy[b]	Fe	4NH	4CH	2N	2C	2S	C_{2h} level	energy[b]	Fe	4NH	4CH	2N	2C	2S	C_{2v} level	NH	CH	$C_{\infty v}$ level	N	C	S
$(2a_u)$	−0.0978		26	74				−0.0920		25	75				$(9a_u)$	−0.1176	0	25	75	0	0	0	$2a_2$ C–N π*	30	70				
$(5b_{2g})$	−0.0984	2	30	65	0	0	2	−0.0926	2	23	74	0	0	0	$(16a_g)$	−0.1185	3	22	71	0	1	2							
$(5b_{3g})$	−0.2059	9	50	41	0	0	0	−0.2216	7	50	43	0	0	0	$(9b_g)$	−0.2274	10	50	40	0	0	0	$2b_2$ C–N π*	57	43				
$(6b_{1u})$	−0.2159	0	49	49	1	0	0	−0.2306	0	49	50	1	0	0	$(12b_u)$	−0.2376	0	49	47	0	0	4							
$(5b_{1g})$	−0.2024	75	24	1				−0.2076	73	26	2				$(10b_g)$	−0.2204	73	25	1	0	0	0				Fe dσ			
$(11a_g)$	−0.2047	76	9	0	13	2	0	−0.2124	75	10	1	13	2	0	$(15a_g)$	−0.2410	56	6	0	6	0	31							
$4b_{2g}$[e]	−0.2521	9	0	0	17	0	74	−0.2657	11	0	0	17	1	72	$12a_g$	−0.3687	19	1	0	45	28	8				2π	30	4	65
$4b_{3g}$	−0.2522	8	0	0	17	0	75	−0.2658	9	0	0	17	1	73	$8b_g$[e]	−0.3194	31	1	1	19	5	43							
$6b_{3u}$	−0.2574	0	0	0	16	0	83	−0.2714	0	0	0	16	0	83	$11b_u$	−0.3422	4	0	2	38	15	42							
$7b_{2u}$	−0.2576	0	0	0	16	0	83	−0.2712	0	0	0	16	0	83	$8a_u$	−0.3317	0	1	0	34	11	54							
$3b_{2g}$	−0.3136	81	4	3	0	4	7	−0.3209	78	6	4	0	3	9	$14a_g$	−0.3398	86	7	5	0	0	1				Fe dπ			
$3b_{3g}$	−0.3205	80	0	7	1	5	8	−0.3278	80	0	6	1	4	9	$7b_g$	−0.3574	64	0	9	13	6	8							
$10a_g$	−0.3243	99	0	1	0	0	0	−0.3320	99	1	0	0	0	0	$13a_g$	−0.3462	97	1	1	1	0	0							
$2b_{2g}$	−0.3894	1	30	9	33	21	7	−0.3928	0	36	10	28	19	8	$10a_g$	−0.4606	27	21	4	4	6	38				1π	35	33	32
$6b_{2u}$	−0.3929	0	6	1	50	31	11	−0.3999	0	8	2	48	30	12	$7a_u$	−0.4144	0	10	2	22	23	42							
$5b_{3u}$	−0.3938	0	6	0	51	32	11	−0.4008	0	7	1	50	31	12	$10b_u$	−0.4185	3	4	6	19	21	48							
$2b_{3g}$	−0.3999	8	5	8	46	26	8	−0.4060	6	7	9	44	25	9	$6b_g$	−0.4148	2	4	5	23	24	43							
$1a_u$	−0.4077		79	21				−0.4036		80	20				$6a_u$	−0.4298	0	74	18	2	3	3	$1a_2$ C–N π	76	24				
$1b_{2g}$	−0.4380	19	45	9	18	7	1	−0.4390	21	36	7	23	10	2	$11a_g$	−0.4362	17	44	10	2	3	24							
$5b_{1u}$	−0.4563	0	48	39	9	1	1	−0.4529	0	51	40	7	1	0	$7b_u$	−0.4911	3	56	31	1	1	9	$1b_2$ C–N π	51	49				
$1b_{3g}$	−0.4766	10	51	33	5	2	0	−0.4744	11	49	31	7	2	0	$5b_g$	−0.4996	10	52	32	0	0	5							
$9a_g$	−0.4772	0	0	0	1	20	80	−0.4978	10	18	16	1	11	45	$7a_g$	−0.5842	6	1	2	1	23	66				3σ	8	25	68
$4b_{1u}$	−0.4779	0	1	1	1	19	79	−0.4986	0	0	0	1	19	79	$6b_u$	−0.5760	2	2	1	1	24	71							
$5b_{2u}$	−0.4552	9	60	26	4	1	0	−0.4534	9	59	26	5	2	0	$5a_u$	−0.4716	9	58	30	0	0	3	$5a_1$ N lp	72	28				
$8a_g$	−0.4990	20	42	37	1	0	0	−0.4982	11	23	21	0	9	36	$8a_g$	−0.5150	17	37	44	0	0	2							
$4b_{3u}$	−0.4662	9	79	8	3	1	0	−0.4644	9	78	8	4	1	0	$8b_u$	−0.4820	8	75	13	2	1	2	$4b_1$ N lp	91	9				
$4b_{1g}$	−0.5247	33	57	10				−0.5255	34	56	10				$4b_g$	−0.5444	33	54	12	0	0	0							
$3b_{1u}$	−0.5578	10	4	1	76	7	1	−0.5660	10	3	1	78	7	0	$9b_u$	−0.4730	0	1	0	88	9	1				4σ	77	14	9
$7a_g$	−0.6048	23	4	13	55	5	0	−0.6118	22	7	19	48	4	0	$9a_g$	−0.4716	0	0	0	90	9	1							

[a] Note that the levels are only roughly in order of decreasing energy. For $Fe(N_2C_2H_4)_2(NCS)_2$ they are grouped by type, in order of decreasing energy within each type. Corresponding levels of $Fe(N_2C_2H_4)_2L_2^+$, L = NCS^-, SCN^-, are listed on the same line without regard to relative energies. [b] 0.11 and −0.06 hartree have been added to all computed energies of $Fe(N_2C_2H_4)L_2^+$, L = NCS^-, SCN^-, to make the energies of the $N_2C_2H_4$ $1a_1$- and $1b_1$-like levels coincident in the three complexes. [c] For energies of these levels in the free ligands, see Figure 1. [d] *Relative* amounts of charge within the atomic spheres. [e] The highest occupied level, containing only one electron for the charged complexes. Symbols for empty levels appear in parentheses.

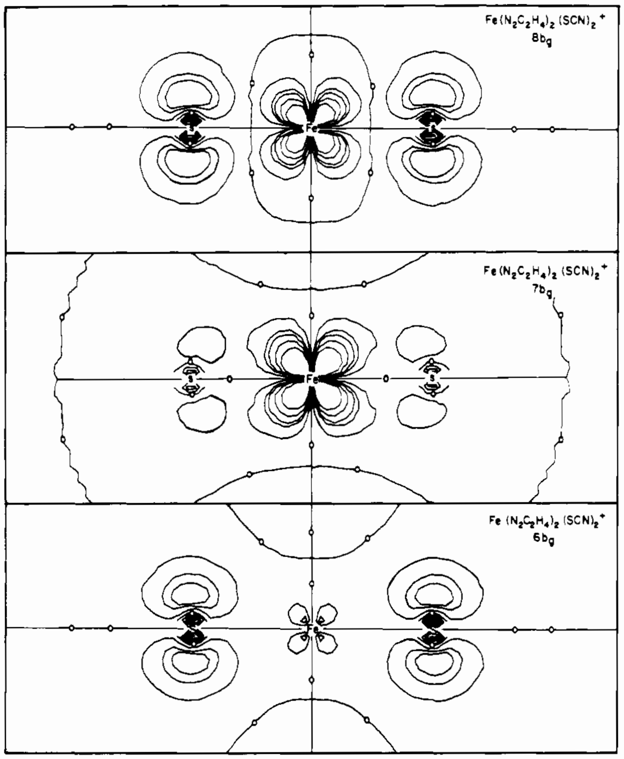

Figure 5. Contour maps of the orbital wavefunctions of $Fe(N_2C_2H_4)_2(SCN)_2^+$ in the *yz* plane which are mainly 1π, Fe $d\pi$, and 2π. The last, $8b_g$, contains the unpaired electron. Note that the carbon and nitrogen atoms of the SCN ligands are not in this plane.

and 2π-like orbitals occur when NCS^- switches from N to S coordination. These are illustrated in greatly oversimplified form by the diagram

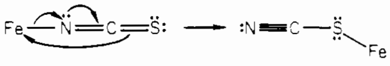

That is, a 1π-like N–C–S bonding orbital ($2b_{2g}$) correlates with the main Fe–SCN σ-bonding orbital ($10a_g$); it is this acquisition of Fe–S bonding character which so stabilizes $10a_g$ below the other 1π-like orbitals in the S-bonded complex (see Figures 2 and 4). A 2π lone pair ($4b_{2g}$) correlates with the new third component of the NCS^- C–N bond ($12a_g$); again, the extra bonding character thus acquired stabilizes $12a_g$ to lower energy than the other 2π-like orbitals. Thus, as seen by comparing Figures 4 and 5, the 1π- and 2π-like orbitals of g symmetry in the *xz* plane are no longer similar to their counterparts in the *yz* plane.

The stabilization of $12a_g$ changes the HOMO from the *xz* to the *yz* 2π-like orbital ($8b_g$, shown in Figure 5). This is, however, an artifact of erroneously placing the $Fe(SCN)_2$ unit in *xz*. Had it been correctly oriented in *yz*, as in the actual crystal structure, very similar orbitals with very similar energies to those which now maximize in *xz* would appear in *yz* and vice versa. Our confidence in this assertion is based on the lack of significant $N_2C_2H_4$ character in any of the 2π-like orbitals.

Reasons for S Coordination of NCS^- in $Fe(N_2C_2H)_4(SCN)_2^+$. The calculations suggest a possible reason and mechanism for the easy interconversion between N- and S-coordinated forms of the oxidized complex. Figure 6 shows a simplified MO diagram for the 1π, $d\pi$, 2π, and $d\sigma$ orbitals, correlated with an electron dot structure, for iron interacting with one NCS^-. Oxidation removes a mainly NCS^- 2π electron, creating radical character on S. This configuration is Jahn–Teller unstable because of the near degeneracy[18] of the two 2π orbitals. The Jahn–Teller theorem will be satisfied if the system distorts so that the iron atom no longer interacts equivalently with these two orbitals. A way to do this which maintains maximum orbital overlap along the whole path is for the thiocyanate to move from σ to π coordination.

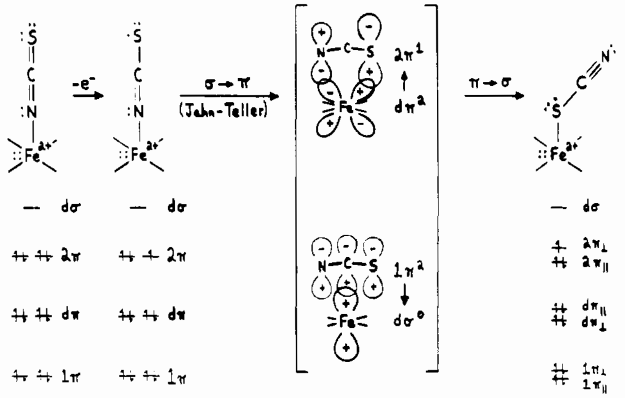

Figure 6. A possible mechanism for conversion from N to S bonding of thiocyanate upon oxidation of $FeTIM(NCS)_2$, illustrated for iron bonded to one thiocyanate.

The main bonding interaction in this intermediate is donation from 1π to $d\sigma$; there is also the possibility of $d\pi$ to 2π donation. Subsequent π to σ conversion gives the S-bonded form, with the 2π degeneracy still lifted because of the bent conformation preferred by S-bonded thiocyanate. One may similarly explain the recent experimental observation that flash photolysis of $FeTIM(NCS)_2$ produces transients which apparently contain both N- and S-bonded thiocyanate:[12] the photoexcitation presumably also removes electrons from the 2π-like orbitals.

It should be noted that the estimated Jahn–Teller preference for the S- over the N-bonded form, as measured by half the $8a_u$–$8b_g$ splitting in Figure 2, is small (4 kcal/mol). Considering that other factors may be significant in the relative stability, e.g., the difference between Fe–N and Fe–S bonding noted above, it is therefore not surprising that both N- and S-bonded forms are observed, depending on conditions.

Fe–$N_2C_2H_4$ π Interactions. Figure 1 suggests the possibility of significant Fe $d\pi \rightarrow N_2C_2H_4$ π^* back-donation, since the C–N π^* orbitals of $N_2C_2H_4$ have comparable energies to the Fe 3d manifold. This is borne out by the actual calculations on the complexes. The $d\pi$ orbitals belong to b_{2g} and b_{3g} in D_{2h}. One would expect the major back-donation to occur in b_{3g}, since the C–N π^* orbital there ($5b_{3g}$) is *C–C* bonding and therefore much lower in energy than its *C–C* antibonding counterpart ($5b_{2g}$). Indeed, $5b_{3g}$ lies 0.01 hartree higher in energy than its noninteracting $6b_{1u}$ partner, while $5b_{2g}$ and $2a_u$ are separated by only 0.0006 hartree. Similarly, $5b_{3g}$ has 9% Fe character in the neutral complex (7% in the N-bonded cation), while $5b_{2g}$ is only 2% Fe. The *bonding* orbital for the back-donation, $3b_{3g}$, is indeed lower in energy than $3b_{2g}$ and has 6–7% $N_2C_2H_4$ character, all on the *carbon* atoms. This is as expected if the $N_2C_2H_4$ character results from back-donation, since $3b_{3g}$ is about equidistant from the C–N π and C–N π^* orbitals of the same symmetry and hence should mix about equally with each of them; the net result of such a three-orbital mixing is to eliminate nitrogen character in the middle, i.e., mainly $d\pi$, orbital. Entirely analogous comments apply to the C_{2h} complex. The conclusion is that there is present Fe $d\pi \rightarrow N_2C_2H_4$ π^* back-donation of about 0.1 electron per $N_2C_2H_4$ ligand, mainly into the C–N π^* orbital which is C-C bonding, in all three complexes. This amount

---

[18] The calculated separation of the 2π-like $4b_{2g}$ and $4b_{3g}$ orbitals in $Fe(N_2C_2H_4)_2(NCS)_2$ is 0.000096 hartree, or 0.06 kcal/mol.

is essentially the same estimated by experiments and other calculations for other α-diimine complexes.[9] It is certainly a significant amount for Fe(II) but does not correspond to a *major* role for resonance structures with multiple Fe–N bonds.

It is interesting to note that the prediction of Figure 2, on the face of it, is that the electron added upon *reduction* of FeTIM(NCS)$_2$ would go into a mainly TIM C–N π^* rather than into an Fe dπ orbital, thus forming an Fe(II)–TIM radical anion complex. Although we know of no well-characterized iron complexes of this sort, a number of "Ni(I)" complexes of conjugated macrycyclic ligands have been shown experimentally to contain in fact Ni(II) and ligand radical anions.[19]

On the basis of these results, one is led to speculate that the HOMO's of FeTIM(MeOH)$_2^{2+}$ might indeed have considerable ligand character, through interaction of the Fe dπ and oxygen-localized MeOH lone-pair orbitals. A calculation on Fe(N$_2$C$_2$H$_4$)$_2$(MeOH)$_2$ itself would be worthwhile due to its catalytic function. We hope eventually to deal with the subtle question of how TIM, as opposed to other neutral macrocycles which set up strong ligand fields, conveys special properties to these systems.

Acknowledgment. We are grateful to E. O. Fey, R. R. Gagné, M. Maroney, and L. Noodleman for discussions and communication of results. We thank the National Science Foundation for support.

Registry No. **2**, 76705-28-7; **2**$^+$, 76705-29-8; **3**$^+$, 76705-30-1; N$_2$C$_2$H$_4$, 40079-19-4; NCS$^-$, 302-04-5; FeTIM(NCS)$_2$, 69765-88-4.

---

[19] Gagné, R. R.; Ingle, D. M. *J. Am. Chem. Soc.* **1980**, *102*, 1444 and references therein.

Contribution from the Department of Chemistry,
Rutgers University, New Brunswick, New Jersey 08903

Intercalation Compounds of FeOCl: Systematics of Nitrogen-Containing Lewis Base Intercalants

ROLFE H. HERBER* and YONEZO MAEDA

Received August 5, 1980

Ten nitrogen-containing Lewis base intercalates of iron(III) oxychloride, FeOCl(G)$_n$, have been prepared and characterized by elemental analysis, powder pattern X-ray diffraction, and ^{57}Fe Mössbauer and Fourier transform infrared spectroscopies. The unit cell *b*-axis expansion confirms the location of the "guest" molecule within the van der Waals layer of the FeOCl lattice, and the magnitude of this expansion provides information concerning the orientation of the intercalant within this layer. The magnetic ordering temperature of FeOCl (90 ± 2 K) is depressed in the intercalates to temperatures below ~78 K. The magnitude of the magnetic hyperfine field in the low-temperature limit (4.2 K) is about 2% larger in the pyridine, ammonia, 2-picoline, and butylamine intercalates than it is in unintercalated FeOCl. The sign of the EFG tensor at the iron atom is a function of stoichiometry rather than dependent on the bonding and structural parameters of the intercalant per se. The Fourier transform infrared spectra of several of the intercalates have been examined in detail and show that a number of fundamental modes—especially those involving ring-breathing modes of the "guest" species—are strongly suppressed in the intercalate.

Introduction

FeOCl is a layered compound belonging to the orthorhombic space group *Pmnm* (D_{2h}^{13}) with 2 formula units per unit cell.[1,2] The crystal structure consists of a stack of double sheets of *cis*-FeCl$_2$O$_4$ octahedra, linked together with shared edges. The unit cell dimensions are $a = 3.780$, $b = 7.917$, and $c = 3.302$ Å. Of particular significance is the fact that the chlorine atoms lie on a plane which defines the edge of each layer, and the bonding across these chlorine atom planes is assumed to be of the van der Waals type. The van der Waals interaction is easily disrupted, and the intercalation of a wide variety of amine bases has been observed to occur under relatively mild conditions.[3,4] The orientation of the intercalated molecular species has been the subject of extensive study, and the *b*-axis expansion of the unit cell as derived from X-ray powder pattern data has been used to elucidate the steric relationships between the guest molecule and the host lattice.

A large number of different Lewis bases including ammonia,[3] pyridine and pyridine derivatives,[5-8] phosphine, and phosphite[9] have been successfully intercalated into FeOCl. It has been observed that, while nonstoichiometric iron(III) oxychloride is capable of intercalating a large number of molecules having Lewis base character, studies of stoichiometric FeOCl base intercalates have so far focused on pyridine and its derivatives as "guest molecules". A lithium intercalate, FeOClLi$_x$ ($x = 0.50$), has been reported by Palvadeau et al.[4] The FeOCl intercalation of two cyclopentadienyl organometallic compounds has been reported by Halbert et al.[10]

In the present study, ten intercalation compounds in which nitrogen-containing Lewis bases are present as guest molecules (G) in an FeOCl host matrix have been prepared, and the hyperfine interactions, lattic dynamics, and vibrational spectra of the systems FeOCl(G)$_n$ are discussed in detail.

Experimental Section

(a) Sample Preparation. Iron(III) oxychloride was prepared from Fe$_2$O$_3$ and FeCl$_3$ by the usual sealed-tube technique discussed in the literature[6-8] and was characterized by colorimetric iron determination and X-ray powder patterns. The intercalates listed in Table I were obtained by soaking FeOCl in the amine base (if a liquid) or in the base dissolved in a suitable solvent. Careful attention was paid during

---

[1] Goldsztaub, S. *C. R. Hebd. Seances Acad. Sci.* **1934**, *198*, 667; *Bull. Soc. Fr. Mineral. Cristallogr.* **1935**, *58*, 6.

[2] Lind, M. D. *Acta Crystallogr., Sect. B* **1970**, *B26*, 1058.

[3] Hagenmuller, P.; Portier, J.; Barbe, B.; Bouclier, P. *Z. Anorg. Allg. Chem.* **1967**, *355*, 209.

[4] Palvadeau, P.; Coic, L.; Rouxel, J.; Portier, J. *Mater. Res. Bull.* **1978**, *13*, 221.

[5] Herber, R. H.; Maeda, Y. "Proceedings of the Conference on Nuclear and Electron Resonance Spectroscopies Applied to Materials Science"; Kaufmann, E. N., Shenoy, G. K., Eds.; North-Holland Publishing Co.: Amsterdam, in press.

[6] Kanamaru, F.; Yamanaka, S.; Koizumi, M.; Nagai, S. *Chem. Lett.* **1974**, 373.

[7] Kikkawa, S.; Kanamaru, F.; Koizumi, M. *Bull. Chem. Soc. Jpn.* **1979**, *52*, 963.

[8] Kanamaru, F.; Shimada, M.; Koizumi, M.; Takao, M. Takada, T. *J. Solid State Chem.* **1973**, *7*, 297.

[9] Herber, R. H.; Maeda, Y. *Inorg. Chem.* **1980**, *19*, 3411.

[10] Halbert, T. R.; Johnston, D. C.; McCandlish, L. E.; Thompson, A. H.; Scanton, J. R.; Dumesic, J. A. *Physica B+C* **1980**, *99B+C*, 128. T. R. Halbert and J. R. Scanlon, *Mater. Res. Bull.* **1979**, *14*, 415.